SciMedCentral

Journal of Radiology & Radiation therapy

Research Article

Effects of Carbon Ion Irradiation via Periostin on Breast Cancer Cell Invasion of the Microenvironment

Preeyaporn Srimawong[1,4]*, Masahiko Sawajiri[1], Hiroaki Terato[2], Kouichi Maruyama[3], and Keiji Tanimoto[1]

[1]*Department of Oral and Maxillofacial Radiology, Hiroshima University, Japan*
[2]*Analytical Research Center for Experimental Sciences, Saga University, Japan*
[3]*Research Center for Radiation Protection, National Institute of Radiological Sciences, Japan*
[4]*Department of Oral and Maxillofacial Radiology, Mahidol University, Thailand.*

***Corresponding author**
PreeyapornSrimawong, Department of Oral and Maxillofacial Radiology, Faculty of Dentistry, Mahidol University, Yothi Street 6, Ratchathewi10400 Bangkok, Thailand, Tel: 66220078378; Fax: 6622007836; Email: preeyaporn.sri@mahidol.ac.th

Submitted: 06 July 2016

Accepted: 20 September 2016

Published: 22 September 2016

ISSN: 2333-7095

Keywords

- Carbon ion radiotherapy
- Breast cancer
- Bone
- Periostin

Abstract

Radiation therapy is effective for pain and local control. However, it has some associated problems such as increased bone metastasis after irradiation and side effects to the surrounding normal bone. Over expression of periostin has been observed in bone metastatic cancer. Many studies have indicated that periostin plays an important role in bone metastasis. However, the role of periostin in the microenvironment of bone invaded by destructive cancer cells remains unclear. It has been reported that expression of periostin is significantly enhanced in bone tissues requiring reconstruction. High LET radiation therapy induces bone hyperplasia and calcification in the irradiated area. In this study, after exposure to gamma-ray and carbon ion irradiation, FM3A/R cells were co cultured with non-irradiated MC3T3-E1 cells. The expression of various bone maturation and metabolic factors in MC3T3-E1 cells was evaluated by RT-PCR or western blotting during a time course. Furthermore, Runx2, OSX, OPN, and OCN were evaluated in MC3T3-E1 cells. The expression levels of these calcification and bone formation cytokines in MC3T3-E1 cells were enhanced by co culture with carbon ion-irradiated FM3A/R cells in the early stage. Radiation therapy for bone metastatic cancer, especially carbon ion beam therapy, has excellent cell-killing effects, and also causes less bone resorption in the radiation field than that observed for gamma-ray irradiation. The differentiation and maturation of osteoblasts might be promoted by periostin stimulation. It can be expected that combined treatment with both carbon ion irradiation and periostin inhibitor administration might become a treatment of choice.

ABBREVIATIONS

RT: Radiotherapy; HIMAC: Heavy Ion Medical Accelerator in Chiba; LET: Linear Energy Transfer; Runx2: Runt-related transcription factor 2; OSX: Osterix; OPN: Osteopontin; OCN: Osteocalcin

INTRODUCTION

Radiotherapy (RT) is a widely used treatment option in cancer. However, recent evidence suggests that doses of ionizing radiation delivered inside the tumor target volume can promote tumor invasion and metastasis, indicating that recurrences will occur after radiotherapy [1,2]. The Heavy Ion Medical Accelerator in Chiba (HIMAC) has been used to perform cancer therapy. Hadron therapy-induced modifications of the tumor microenvironment may contribute to the therapeutic effects of radiotherapy. Heavy ion RT is a synonym of carbon ion therapy in current clinical practice [3].

High-energy transfer treatment using a heavy ion beam provides better local control of various types of primary cancers than conventional photon irradiation [4].Carbon ion RT has been performed for radio-resistant tumors in the head and neck region. Reports of carbon ion RT on the treatment of radio-resistant malignancies in the head and neck region such as sarcoma, adenoid cystic carcinoma (ACC) and melanoma have demonstrated therapeutic effectiveness without severe morbidity of the normal tissues. [5-7].The advantages of heavy ion irradiation for cancer arise because of its unique physical properties. High-energy release from a charged particle ion

beam at the end of the beam path (Bragg peak) enables precise targeting of the margins of tumors and can transfer the energy to tumors located deep inside the body, thereby avoiding energy loss at the body surface. This type of energy transfer also causes less chromosomal damage in normal tissues compared with that caused by photon irradiation [8,9] and it is noteworthy that the tumor cell death caused by heavy ion irradiation was reported to be mainly mediated by double-stranded DNA breaks [10,11]. It is also noteworthy that, unlike photon irradiation, particle irradiation may suppress the metastatic potential of cancer [12]. Recently, there have been several controversial reports regarding the effects of radiotherapy on the host immune response to tumors. For example, some groups have demonstrated that photon-beam irradiation enhances tumor metastasis [13,14]. Previous studies reported increased serum periostin levels in breast cancer patients with bone metastases [15,16].

Partial carbon ion irradiation of the body induces bone responses that are qualitatively and quantitatively different from those induced by an equivalent dose of gamma-ray irradiation [17]. Calcification occurs after carbon ion irradiation in radiotherapy of bone and soft-tissue tumors [18]. Conventionally, in carbon ion radiation therapy for bone invasive tumors, bone resorption is decreased, and pathological fractures following irradiation are suppressed. In animal experiments, carbon ion irradiation has been shown to induce calcification and bone formation in irradiated bone trabeculae [17].

Periostin can directly interact with collagen I, fibronectin, and bone morphogenetic protein (BMP)-1. Periostin can recruit BMP-1 onto the fibronectin matrix to promote lysyl oxidase activity for collagen [19,20]. Periostin, originally isolated as an osteoblast-specific factor, is a disulfide-linked 90-kD secretory protein that functions as a cell adhesion molecule for pre-osteoblasts and is involved in osteoblast recruitment, attachment, and spreading [21]. Periostin was originally identified in a mouse osteoblastic library [22].

It has been deduced that when bone invasive cancer cells are injured by carbon ion irradiation, the surrounding bone metabolism and bone osteoblasts are stimulated by irradiated cancer cell-produced periostin, transforming growth factor (TGF)-β, and other cytokines. In this study, the potential causes of the increases in bone mass and differentiation and maturation of osteoblasts were investigated

The role of periostin in bone metabolism after tumor radiotherapy was focused upon. In the bone invasion microenvironment, we evaluated periostin after carbon ion or gamma-ray irradiation and carried out the following experiments, because it is known that periostin is highly expressed in bone invasive cancers, such as breast cancer. The expression levels of periostin related to bone metabolism according to the dose of carbon ion or gamma-ray irradiation were investigated. After exposure to carbon ion or gamma-ray irradiation, bone invasive breast cancer cells were cultured with MC3T3-E1 cells in invasion assays, and measured for their periostin expression by RT-PCR. The cytokines produced by MC3T3-E1 cells were evaluated by western blotting. Irradiated FM3A/R breast cancer cells were also transplanted into mice, and the metastatic area and invaded bone were observed by immunohistochemical assays.

MATERIALS AND METHODS

Cell culture

FM3A/R breast cancer cells were kindly provided by the Cell Resource Center for Biomedical Research, Institute of Development, Aging and Cancer, Tohoku University, and grown in RPMI-1640 medium (Invitrogen, Carlsbad, CA, USA) supplemented with 10% (v/v) charcoal-stripped FBS (Gibco, New York, NY, USA), 100 U/mL penicillin, and 100 μg/mL streptomycin (Gibco, Palo Alto, CA, USA) under 5% (v/v) CO_2 in air at 37°C. MC3T3-E1 osteoblastic cells derived from the calvarias of newborn C57BL/6 mice were obtained from the Riken Cell Bank(Tsukuba, Japan). MC3T3-E1 cells were cultured in MEMα (Invitrogen, St. Louis, MO, USA) supplemented with 10% charcoal-stripped FBS, 100 U/mL penicillin, and 100 μg/mL streptomycin at 37°C in an atmosphere of 5% (v/v) CO_2 in air.

Irradiation

FM3A/R cells were seeded into 50-mL cell culture flasks (Falcon® 25 cm^2 Flask; Corning Inc. Life Sciences, Tewksbury, MA, USA)at approximately 5 × 10^4 cells/flask, grown to near confluence (2 or 3 days after seeding), and then exposed to carbon ion or gamma-ray irradiation. Carbon ion irradiation was carried out using a MONO peak carbon ion beam at the Heavy Ion Medical Accelerator, National Institute of Radiological Sciences (Chiba, Japan). The estimated linear energy transfer averaged 40 KeV μm^{-1}, and the dose rate was 3 Gy min^{-1}. The beam intensity was measured using dose monitors installed in the beam path. Binary filters made of poly (methyl methacrylate) plates (0.5–128-mm thickness) were used to adjust the linear energy transfer. Gamma-ray irradiation was performed at a dose of 1 Gy min^{-1} using a GammaCell® 40 Exactor (Best Theratronics Ltd., Ottawa, ON, Canada).

Coculture assay in vitro

To determine whether periostin secretion by breast cancer cells affects osteoblastic cell metabolism, BD Falcon™ Cell Culture Inserts with 4-μm pores (Falcon/Becton Dickinson, Franklin Lakes, NJ, USA) were used. Briefly, after trypsinization, 5 × 10^5 MC3T3-E1 cells were resuspended in the lower compartment with 2.0 mL of MEM α medium and incubated under 5% (v/v) CO_2 in air at 37°C for 24 h. Next, 5 × 10^5 irradiated or non-irradiated FM3A/R cells were suspended in the upper compartment with 2.0 mL of RPMI-1640 medium immediately after irradiation, and the upper compartment was placed in the lower compartment of the cell culture dish. Co culture was performed until the end of the experimental period under 5% (v/v) CO_2 in air at 37°C. The FM3A/R cells and MC3T3-E1 cells were evaluated at days 3, 5, and 7 post-irradiation. The FM3A/R cells in the upper compartment were evaluated by RT-PCR assays and the MC3T3-E1 cells in the lower compartment were evaluated by western blotting.

RT-PCR and real-time PCR

Total RNA was prepared using RNAiso Plus (Takara Bio, Shiga, Japan) in accordance with the manufacturer's instructions. First-strand cDNAs were synthesized for RT-PCR using a RevertraAce qPCR RT Kit (Toyobo, Osaka, Japan) following the manufacturer's protocol. Real-time quantitative RT-PCR was carried out using

Dynamo polymerase (Thermo, Waltham, MA, USA) and an ABI Prism 7700 Sequence Detection System (Applied Biosystems, Foster City, CA, USA). The relative amounts of periostin mRNA was normalized to the amounts of GAPDH mRNA in the same samples. The PCR amplifications for these mRNAs were performed using the primer pairs shown in Table (1). The amplification parameters were as follows: initial denaturation at 95°C for 1 min; and 40 cycles of denaturation at 95°C for 15 s and extension at 60°C for 60 s.

Western blot analysis

For western blot analysis, cells were lysed in lysis solution comprised of Pierce® RIPA buffer,Halt™ Protease and Phosphatase Inhibitor Cocktail, and 0.5 M EDTA Solution (all from Thermo Scientific Inc.; Rockford, IL, USA). The protein concentrations of the lysates were determined by the Bradford protein assay. Next, aliquots (15 μg protein) were separated by SDS-PAGE using 10–20% gel concentrations (ATTO Corp., Tokyo, Japan) and transferred to Immobilon®-P transfer membranes (EMD Millipore Corp., Billerica, MA, USA). After blocking in 3% nonfat skim milk (Wako Pure Chemical Industries, Osaka, Japan) in TBS-T (10 mMTris-HCl pH 8.0, 0.05% Tween-20) for 1.5 h at room temperature, the membranes were incubated with anti-Runt-related transcription factor 2 (Runx2), anti-osterix (OSX), anti-OPN, and anti-osteocalcin (OCN) primary antibodies (all from Santa Cruz Biotechnology, Santa Cruz, CA, USA) diluted 1:200 in TBS-T overnight at 4°C. The membranes were then washed with TBS-T, incubated with anti-mouse or anti-rabbit horseradish peroxidase-conjugated secondary antibodies (GE Healthcare, Little Chalfont, UK; 1:3000 in TBS-T) for 1 h at room temperature, and washed in TBS-T. The signals were visualized with an enhanced chemiluminescence solution (GE Healthcare, Little Chalfont, UK) and analyzed using a ChemiDoc™ XRS+ System with Image Lab™ Software (Bio-Rad Laboratories Inc., Hercules, CA, USA).

Transplantation assay in mice

To examine whether periostin expression in FM3A/R cells affects their growth and invasion *in vivo*, irradiated FM3A/R cells (1×10^4 in 100 μL of normal saline) were injected into the tibiae of mice. The control mice were injected with the same number of non-irradiated FM3A/R cells. For these experiments, male C57BL/6 mice were obtained from SLC (Shizuoka, Japan), and housed in the animal facility of Hiroshima University. The mice were housed at 4–5 animals/cage in a room with controlled temperature (23°C), humidity (24%), and light/dark cycle (13 h/11 h), and had free access to food and water. All animal experiments were performed in accordance with the Guideline of the Committee of Animal Experimentation, Hiroshima University and the Committee of Research Facilities for Laboratory Animal Science, Natural Science Center for Basic Research and Development (N-BARD), Hiroshima University (Permit Number: A15-96). The animals were monitored for tumor formation every day, and euthanized after 1 month by excessive anesthesia given as an abdominal injection of ketamine and xylazineto minimize suffering. The hind legs of all mice were fixed with 10% buffered formalin, and scanned using a Micro-CT 1176 (SkyScan, Bruker, Belgium) before decalcification. The tumor tissues were decalcified with 10% EDTA, embedded in paraffin, sectioned at 4-μm thickness, and stained with hematoxylin and eosin. Triple staining was carried out by tartrate-resistant acid phosphatase (TRAP) staining and immunostaining with anti-periostin antibodies for histological analysis. Counter staining was performed with methyl green.

RESULTS

RT-PCR assay

The effects of gamma-ray and carbon ion irradiation on FM3A/R breast cancer cells were initially explored. FM3A/R cells were exposed to carbon ion or gamma-ray irradiation, and measured for their expression of periostin after irradiation and at several time points during the time course by RT-PCR. The results from real-time RT-PCR analyses revealed that the mRNA expression of periostin, which is deeply involved with the development of breast cancer, varied dynamically after irradiation (Figure 1). The results showed that irradiation increased periostin mRNA expression in FM3A/R cells after irradiation, but there were no significant differences at days 1 and 3. When the mRNA expression levels were determined at days 5 and 7 post-irradiation, the periostin mRNA level had dramatically increased in gamma-ray-irradiated cells, while the periostin mRNA levels were augmented in 6 Gy carbon ion-irradiated cells. Periostin mRNA expression was not significantly altered at days 5 and 7 after 2 and 4 Gy of carbon ion irradiation. At 3 days after exposure, periostin mRNA expression was higher than that in the non-irradiated control group, and in particular, the gamma-ray-irradiated groups showed higher values than the carbon ion-irradiated groups. Both the carbon ion- and gamma-ray-irradiated FM3A/R cell groups showed remarkable increases in periostin expression at days 5 and 7 post-irradiation.

Western blotting assay

The expression of periostin mRNA in irradiated and non-irradiated FM3A/R cells did not show any significant differences until day 3 post-irradiation in both the carbon ion- and gamma-ray-irradiated groups. Significant differences were appeared from day 5, and the co cultured MC3T3-E1 cells were affected by the changes in periostin expression.

Runx2 in the low-dose irradiation groups showed higher values than those in the non-irradiated group at day 3, but these decreased at day 5. A reduction was evident in the carbon ion-irradiated groups (Figure 2).OSX in both the gamma-ray- and carbon ion-irradiated groups showed increases at days 3 and 7,

Table 1: Primer sequences used for RT-PCR.

Gene	Forward Primer	Reverse Primer
GAPDH	CGGAGTCAACGGATTTGGTCGTAT	AGCCTTCTCCATGTTGGTGAAGAC
Periostin	AATGCTGCCCTGGCTATATG	GTAGTGGCTCCCACAATGC

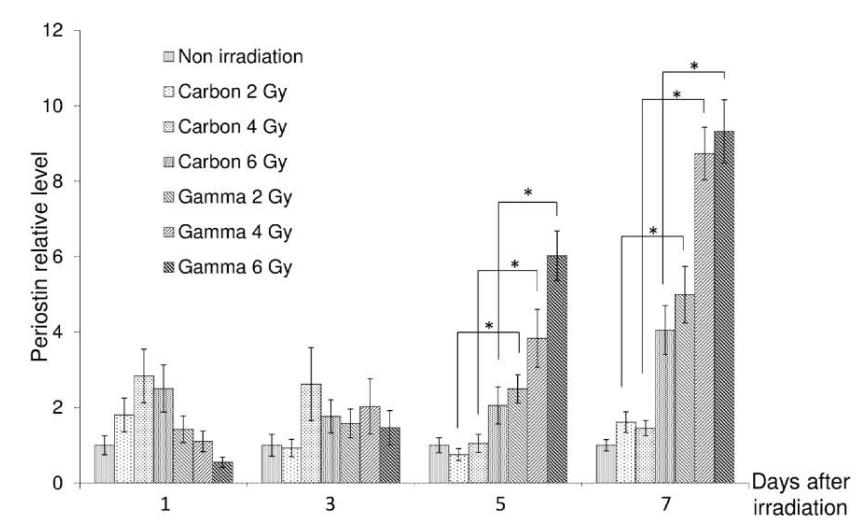

Figure 1 There were no significant differences in periostin expression in the carbon ion- and gamma-ray-irradiated groups until day 3 post-irradiation. After day 5, the gamma-ray-irradiated cells showed a dose-dependent increase in the periostin expression level. The non-irradiated cells are shown as 1 (paired t-test, *P < 0.05 for difference between carbon ion and gamma-ray irradiation). Data represent the means ± SD of three experiments.

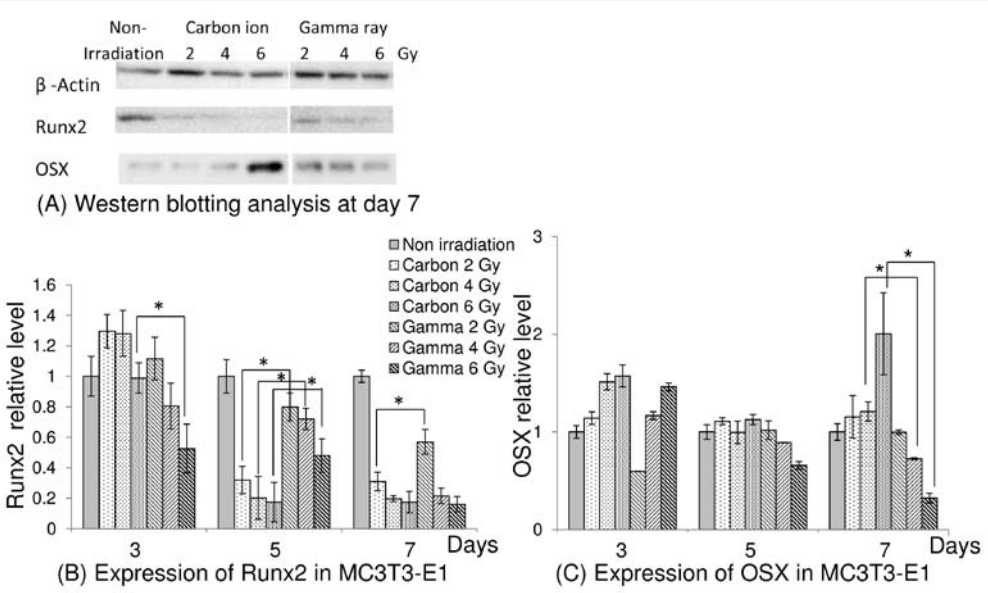

Figure 2 (A) Western blotting analyses at day 7. (B) Runx2 in the carbon ion-irradiated groups was rapidly decreased at day 5 post-irradiation in a dose-dependent manner. (C) Although a decreasing trend was already seen at day 3, the levels in the gamma-ray-irradiated groups declined slowly. OSX increased according to the irradiation dose at day 7 in the carbon ion-irradiated groups. The non-irradiated cells are shown as 1 (paired t-test, *P < 0.05 for difference between carbon ion and gamma-ray irradiation). Data represent the means ± SD of three experiments.

and then declined in the gamma-ray-irradiated groups compared with the non-irradiated group (Figure 2).

The expression of OPN, a protein involved in bone matrix formation, was not greatly influenced by changes in periostin expression at days 3 and 5 post-irradiation. OPN was significantly increased in the 4 and 6 Gy carbon ion-irradiated groups at day 7. Meanwhile, its expression declined to accompany the increase in periostin expression in the gamma-ray-irradiated groups (Figure 3). OCN is a protein involved in calcification. In the high-dose irradiation groups, OCN showed an increase at days 3 and 5 post-irradiation compared with the non-irradiated group. The gamma-ray-irradiated groups showed decreased levels of OCN at day 7. The presence of periostin might promote OCN, but stimulation by excessive periostin was suggested to cause a decrease in OCN (Figure 3).

Transplantation assay in mice

Irradiated and non-irradiated control FM3A/R breast cancer

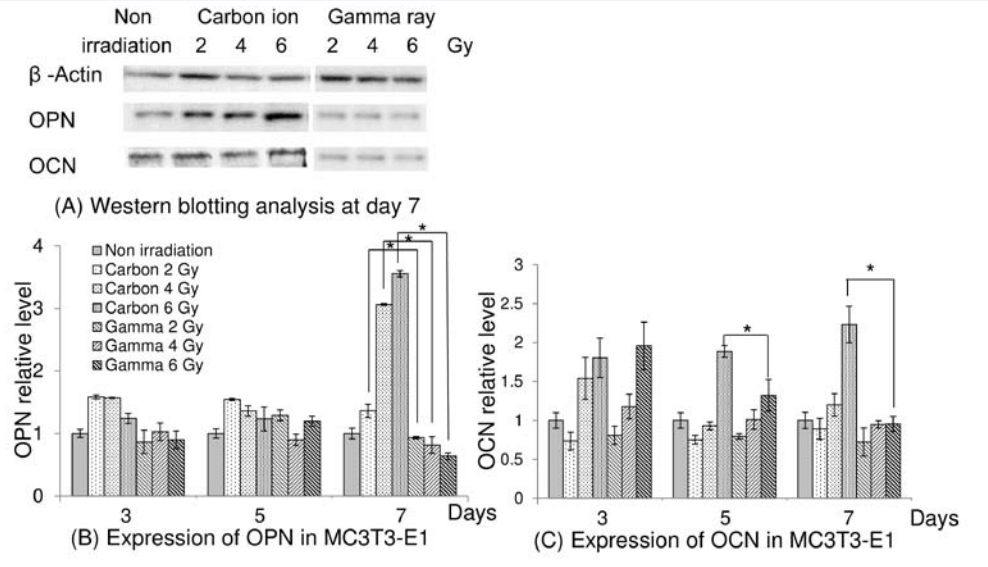

Figure 3 (A) Western blotting analyses at day 7 post-irradiation. The 6 Gy carbon ion-irradiated group expressed strong signals. (B) OPN expression showed no significant differences until day 5 post-irradiation, while the carbon ion-irradiation groups showed large increases at day 7. (C) OCN expression increased compared with the non-irradiated group in a dose-dependent manner. However, the gamma-ray-irradiated groups did not differ significantly from the non-irradiated group, while the high-dose carbon ion-irradiated group showed increases at days 5 and 7. The non-irradiated cells are shown as 1 (paired t-test, *P < 0.05 for difference between carbon ion and gamma-ray irradiation). Data represent the means ± SD of three experiments.

cells were administered as transplanted tumor cells to mice. FM3A/R cells can be engrafted by transition to the tibiae near the knee joint at a relatively high frequency after transplantation. Obvious severe bone destruction was seen on CT images, and the cortical bone had a rough surface (Figure 4A). Microscopic observation showed evidence of bone invasion by the tumors. Osteoclasts were seen at the boundary surface of the bone and tumors. In the vicinity of the carbon ion-irradiated tumor cells, it was observed that the osteoclasts were slightly smaller compared with those in the vicinity of the gamma-ray-irradiated or non-irradiated tumor cells (Figure 4B).

Bone destruction was prominently seen in the bone transplanted with non-irradiated breast cancer cells, but periostin expression was not visible around the non-irradiated cells. Metastatic breast cancer cells were observed to be strongly stained for periostin in gamma-ray- or carbon ion-irradiated cells, and the osteoclasts found in bone resorption lacunae were miniaturized (Figure 4B). Expansion and irregular bone formation were found in the carbon ion-irradiated group (Figure 5).

In the high-magnification images shown in Figure (5) for transplantation of carbon ion-irradiated cells, irregular bone formation was found adjacent to the transplanted area of the irradiated breast cancer cells. Active osteoblastic cells were present between the tumor cells and the irregular bone (Figure 6).

DISCUSSION

Periostin is expressed in many organs and tissues, and should have a variety of roles for its action. Periostin is suspected to be an important factor for bone invasion of cancer and bone metabolism, because its expression is increased or decreased in the microenvironment of cancer bone invasion. However, the roles of periostin are unclear. Heavy ion irradiation is known to be effective for pain control and local control. Periostin is produced by FM3A/R breast cancer cells, and its production is increased by irradiation. In our research, the periostin concentration in the co culture medium should increase after irradiation, suggesting that bone-forming cells adjacent to the tumor might be stimulated by periostin in the microenvironment. To clarify the role of periostin and the effects of irradiation on the bone invasion region, we performed measurements of periostin in breast cancer cells and other bone metabolic proteins in coculture systems to analyze the interactions between tumor cells and osteoblastic cells.

RTis effective for pain control and local control. In particular, heavy particle ion RT is superior in its tumor cell-killing effect. However, it is not clear whether carbon ion irradiation causes different bone responses compared with gamma-ray irradiation, such as bone volume increases in the irradiation field [17,18]. We focused on studying calcification metabolism by bone-forming cells through changes in periostin expression after carbon ion and gamma-ray irradiation for breast cancer cells.

Periostin is produced by FM3A/R breast cancer cells, and its production is increased by irradiation. Periostin produced by bone metastatic FM3A/R breast cancer cells was measured after exposure to carbon ion or gamma-ray irradiation. Expression of periostin was observed to differ significantly between carbon ion and gamma-ray irradiation at days 5 and 7 post-irradiation. The production of periostin in breast cancer cells exposed to gamma-ray irradiation was decreased compared with that in non-irradiated cells, but then increased immediately thereafter. It is suspected that the periostin concentration in the

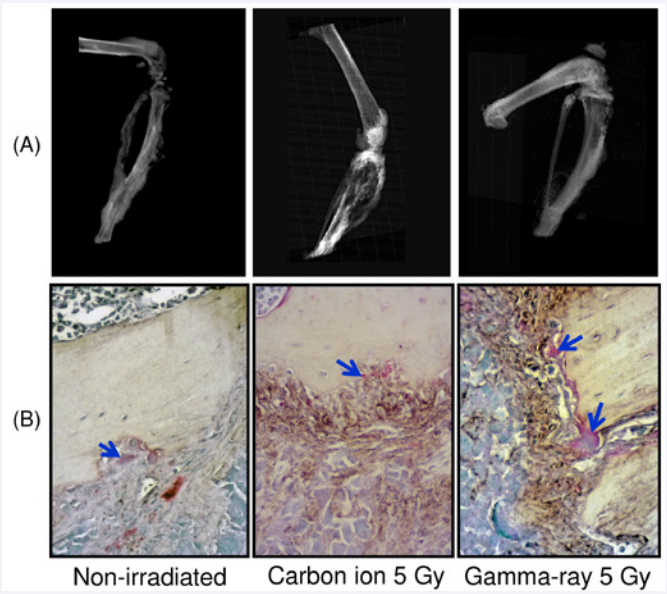

Figure 4 (A) Micro-CT images of non-irradiated cells, 5 Gy carbon ion-irradiated, and 5 Gy gamma-ray-irradiated cells taken from the proximal tibia. The bone surfaces were resorbed and showed a rough surface in all samples. (B) The presence and localization of periostin and other bone metabolic factors were analyzed. Cancer cells and growth of cancer tissues were seen in the bone marrow in all samples. Triple staining for periostin (brown), TRAP (red), and methyl green in high-magnification images is shown. Arrows indicate osteoclastic cells.

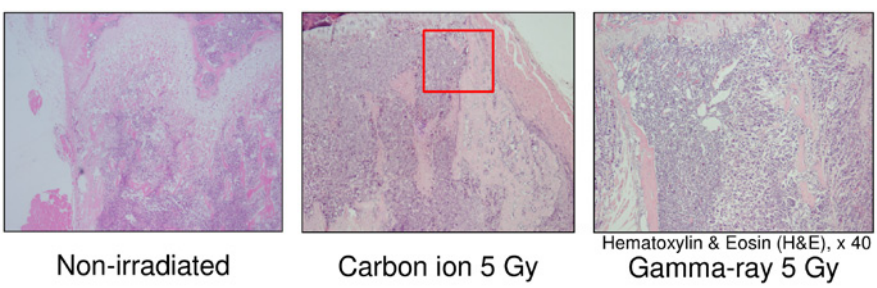

Figure 5 Formation of irregular bone was observed in mice transplanted with carbon ion-irradiated cells. It was suggested that the maturation and differentiation of osteoblasts were affected by periostin production by the irradiated breast cancer cells.

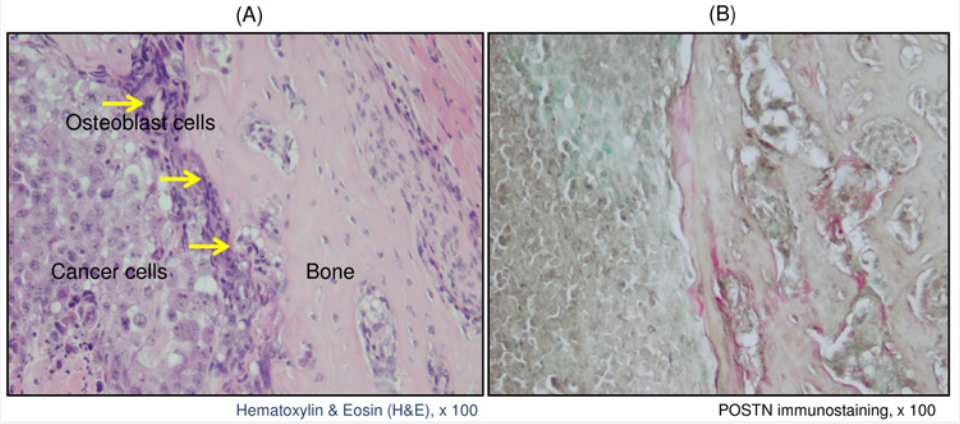

Figure 6 (A) High-magnification images of the red boxed area in Figure 5. Irregular bone formation was found adjacent to the transplanted area of carbon ion-irradiated breast cancer cells. Active osteoblastic cells (arrows) were present between the cancer cells and the irregular bone. (B) In periostin immunostaining, brown-colored cells represent periostin expressing breast cancer cells and red-colored cells represent active osteoclastic cells.

microenvironment of the breast cancer cell metastatic region in gamma-ray irradiated cells was higher than that in non-irradiated cells.

However, higher expression of periostin was observed in the gamma-ray-irradiated cells at day 5 compared with the non-irradiated cells. It was reported that irradiation promotes cancer metastasis and that periostin isincreased in metastatic cancer cells from patients [23]. Further observation showed that the expression of periostin was increased at day 7 depending on the irradiation dose, and particularly that gamma-ray-irradiated cells expressed several times more periostin that non-irradiated control cells. The periostin concentration in the co culture medium should increase, and then MC3T3-E1osteoblastic cells would be stimulated by periostin.

Meanwhile, OPN and OCN expression in MC3T3-E1osteoblasticcellsbecome marked at 1weekafter seeding, and Runx2 and OSX are expressed strongly at 3 weeks in general [24-26].In our co culture experiments, expression of OPN and OCN was observed at day 3. Expression of OCN increased in a dose-dependent manner in both the carbon ion- and gamma-ray-irradiated groups. Differentiation and mineralization were accelerated in osteoblasts, and were suspected to have arisen through the enhanced periostin expression. Expression of periostin in the gamma-ray-irradiated group was higher than that in the carbon ion-irradiated group, while OCN expression in the osteoblastic cells was reduced at day 5.

In the animal experiments, bone destruction occurred after transplanting irradiated or non-irradiated cells, and the irradiated cancer cells strongly expressed periostin, as confirmed by immunostaining. Thus, osteoclasts were miniaturized by carbon ion irradiation, and bone absorption was considered to be suppressed in a previous study [27]. Meanwhile, bone resorption was accelerated by gamma-ray irradiation [27]. It was reported that periostin promoted the growth and differentiation of osteoclasts [28].It was suggested that periostin expression was enhanced by gamma-ray irradiation, and the produced periostin promoted bone resorption by osteoclasts. The bone destruction was also confirmed on CT images. The carbon ion-irradiated group showed tibia expansion, and irregular bone formation was found by histological analysis. There was strong expansion and irregular bone tissue augmentation adjacent to cancer cells, and an active osteoblast layer was present between the irregular bone and the tumor tissue. It can be inferred that the osteoblast activity led to the formation and calcification of a large amount of bone matrix. In the presence of periostin, the bone formation occurred for a long period, and the calcification was enhanced. The gamma-ray-irradiated group exhibited more periostin, but formation of irregular bone was not seen.

To further explain the effects of periostin, its mechanism of action should be elucidated. In a previous study, it was reported that matrix metalloproteinase (MMP)-13 was increased by parathyroid hormone-related protein enhancement in breast cancer cells after gamma-ray irradiation, followed by a decrease in the bone. Periostin was also reported to be a catabolic factor that promoted collagen and proteoglycan degradation through activation of the canonical Wnt pathway and downstream induction of MMP-13 expression. Mechanical loading experiments on mouse bone showed that periostin was up regulated, while sclerostin, a potent antagonist of bone formation through inhibition of Wnt and BMP signaling, was down regulated [29]. It was demonstrated that the periostin-induced downregulation of sclerostin and subsequent activation of Wnt/β-catenin signaling may be implicated in the induced bone loss, allowing us to better understand the mechanisms mediating the osteo protective role [30]. Another report indicated that Wnt/β-catenin signaling controls the fate of pre-osteoblasts, as lineage-committed early osteoblasts, with respect to differentiation into osteoblastic or adipocytic populations in bone [31].Taken together, the presence of excess periostin might promote bone absorption because of osteoblastic hypermetabolism.

In the future, studies are required to investigate the stimulation of other products, such as TGF, and the impacts of radiation on the bone-matrix forming cells. Radiation-induced TGF-β is primarily involved in normal tissue injury and fibrosis. TGF-β could be released from the bone matrix destroyed by cancer cells, and may act as a promoter of cell proliferation and invasion. TGF-β signaling regulates several different biological processes, including cell growth, differentiation, apoptosis, motility, angiogenesis, epithelial–mesenchymal transition, and extracellular matrix production [32]. Furthermore, periostin stimulates the TGF-β signaling pathway, given that overexpressed periostin caused TGF-β-dependent secretion of type 1 collagen in fibroblasts [31].It was suggested that the maturation and differentiation of osteoblasts was affected by periostin overexpression. Radiation therapy for bonemetastatic cancer, especially carbon ion beam therapy, has excellentcell-killing effects, and furthermore bone resorption in the radiation field is less than that after gamma-ray irradiation. It can be expected that combined treatment with both carbon ion irradiation and periostin inhibitor administration might become a treatment of choice.

CONCLUSION

Carbon ion irradiation may reduce the production of bone-destroying cytokines and vascularization factors by osteoblasts in the microenvironment of cancer invasion in bone. Therefore, carbon ion irradiation may be a more effective therapy for cancers capable of invading bone, by suppressing the development of distant metastases. The expression of calcification and bone formation cytokines in MC3T3-E1 cells was enhanced by co culture with carbon ion-irradiated FM3A/R cells in the early stage. The differentiation and maturation of osteoblasts might promoted by periostin stimulation. It can be expected that combined treatment with both carbon ion irradiation and periostin inhibitor administration might become a treatment of choice.

ACKNOWLEDGEMENT

This study was performed as part of, and was partially supported by, the Heavy Ion Medical Accelerator in Chiba (HIMAC) Research Project of the National Institute of Radiological Sciences (NIRS) and the joint usage Research Institute for Radiation biology and Medicine, Hiroshima University.

REFERENCES

1. Barcellos-Hoff MH, Park C, Wright EG. Radiation and the

microenvironment - tumorigenesis and therapy. Nat Rev Cancer. 2005; 5: 867-75.

2. Sofia Vala I, Martins LR, Imaizumi N, Nunes RJ, Rino J, Kuonen F , et al. Low doses of ionizing radiation promote tumor growth and metastasis by enhancing angiogenesis. PLoS One. 2010; 21: 11222.

3. Demizu Y, Fujii O, Iwata H, Fuwa N. Carbon ion therapy for early-stage non-small-cell lung cancer. Biomed Res Int. 2014; 2014: 727962.

4. Schulz-Ertner D, Tsujii H. Particle radiation therapy using proton and heavier ion beams. J Clin Oncol. 2007; 25: 953-64.

5. Koto M, Hasegawa A, Takagi R, Ikawa H, Kamada T. Carbon ion radiotherapy for head and neckcancer. J Radiol Radiat Ther. 2014; 2: 1044.

6. Mizoe JE, Hasegawa A, Jingu K, Takagi R, Bessyo H, Morikawa T , et al. Results of carbon ion radiotherapy for head and neck cancer. Radiother Oncol. 2012; 103: 32-37.

7. Lee R, Yamada S, Yamamoto N, Miyamoto T, Ando K, Durante M , et al. Chromosomal aberrations in lymphocytes of lung cancer patients treated with carbon ions. J Radiat Res. 2004; 45: 195-199.

8. Iwakawa M, Noda S, Yamada S, Yamamoto N, Miyazawa Y, Yamazaki H , et al. Analysis of non-genetic risk factors for adverse skin reactions to radiotherapy among 284 breast cancer patients. Breast Cancer. 2006; 13: 300-307.

9. Murakami M, Eguchi-Kasai K, Sato K, Minohara S, Yatagai F, Kanai T. Differences in heavy-ion-induced DNA double-strand breaks in a mouse DNA repair-deficient mutant cell line (SL3-147) before and after chromatin pro... J Radiat Res. 1995; 36: 258-264.

10. Heilmann J, Taucher-Scholz G, Haberer T, Scholz M, Kraft G. Measurement of intracellular dna double-strand break induction and rejoining along the track of carbon and neon particle beams in water. Int J Radiat Oncol Biol Phys. 1996; 34: 599-608.

11. Ogata T, Teshima T, Kagawa K, Hishikawa Y, Takahashi Y, Kawaguchi A, et al. Particle irradiation suppresses metastatic potential of cancer cells. Cancer Res. 2005; 65: 113-120.

12. Ohuchida K, Mizumoto K, Murakami M, Qian LW, Sato N, Nagai E, et al. Radiation to stromal fibroblasts increases invasiveness of pancreatic cancer cells through tumor-stromal interactions. Cancer Res. 2004; 64: 3215-3222.

13. Wild-Bode C, Weller M, Rimner A, Dichgans J, Wick W. Sublethal irradiation promotes migration and invasiveness of glioma cells: implications for radiotherapy of human glioblastoma. Cancer Res. 2001; 61: 2744-2750.

14. Contié S, Voorzanger-Rousselot N, Litvin J, Clézardin P, Garnero P. Increased expression and serum levels of the stromal cell-secreted protein periostin in breast cancer bone metastases. Int J Cancer. 2011; 128: 352-360.

15. Sasaki H, Yu CY, Dai M, Tam C, Loda M, Auclair D , et al. Elevated serum periostin levels in patients with bone metastases from breast but not lung cancer. Breast Cancer Res Treat. 2003; 77: 245-252.

16. Sawajiri M, Mizoe J. Changes in bone volume after irradiation with carbon ions. Radiat Environ Biophys. 2003; 42: 101-106.

17. Tsujii H, Mizoe JE, Kamada T, Baba M, Kato S, Kato H , et al. Overview of clinical experiences on carbon ion radiotherapy at NIRS. Radiother Oncol. 2004; 73: 41-49.

18. Kudo A. Periostin in fibrillogenesis for tissue regeneration: periostin actions inside and outside the cell. Cell Mol Life Sci. 2011; 68: 3201-3207.

19. Maruhashi T, Kii I, Saito M, Kudo A. Interaction between periostin and BMP-1 promotes proteolytic activation of lysyl oxidase. J Biol Chem. 2010; 285: 13294-13303.

20. Horiuchi K, Amizuka N, Takeshita S, Takamatsu H, Katsuura M, Ozawa H , et al. Identification and characterization of a novel protein, periostin, with restricted expression to periosteum and periodontal ligament and increased expression by transforming growth factor beta. J Bone Miner Res. 1999; 14: 1239-1249.

21. Takeshita S, Kikuno R, Tezuka K, Amann E. Osteoblast-specific factor 2: cloning of a putative bone adhesion protein with homology with the insect protein fasciclin I. Biochem J. 1993; 294 : 271-278.

22. Vicini FA, Kestin L, Huang R, Martinez A. Does local recurrence affect the rate of distant metastases and survival in patients with early-stage breast carcinoma treated with breast-conservi. Cancer. 2003; 97: 910-909.

23. Matsuguchi T, Chiba N, Bandow K, Kakimoto K, Masuda A, Ohnishi T. JNK activity is essential for Atf4 expression and late-stage osteoblast differentiation. J Bone Miner Res. 2009; 24: 398-410.

24. Komori T. Regulation of osteoblast differentiation by Runx2. Adv Exp Med Biol. 2010; 658: 43-49.

25. Komori T. Regulation of bone development and maintenance by Runx2. Front Biosci. 2008; 13: 898-903.

26. Sawajiri M, Mizoe J, Tanimoto K. Changes in osteoclasts after irradiation with carbon ion particles. Radiat Environ Biophys. 2003; 42: 219-223.

27. Gerbaix M, Vico L2, Ferrari SL1, Bonnet N3. Periostin expression contributes to cortical bone loss during unloading. Bone. 2015; 71: 94-100.

28. Bonnet N, Standley KN, Bianchi EN, Stadelmann V, Foti M, Conway SJ, et al. The matricellular protein periostin is required for sost inhibition and the anabolic response to mechanical loading and physical activity. J Biol Chem. 2009; 284: 35939-35950.

29. Lv J, Sun X, Ma J, Ma X, Xing G, Wang Y, et al. Involvement of periostin-sclerostin-Wnt/β-catenin signaling pathway in the prevention of neurectomy-induced bone loss by naringin. Biochem Biophys Res Commun. 2015; 468: 587-593.

30. Song L, Liu M, Ono N, Bringhurst FR, Kronenberg HM, Guo J. Loss of wnt/β-catenin signaling causes cell fate shift of preosteoblasts from osteoblasts to adipocytes. J Bone Miner Res. 2012; 27: 2344-2358.

31. Dancea HC, Shareef MM, Ahmed MM. Role of Radiation-induced TGF-beta Signaling in Cancer Therapy. Mol Cell Pharmacol. 2009; 1: 44-56.

Cite this article

Srimawong P, Sawajiri M, Terato H, Maruyama K, Tanimoto K (2016) Effects of Carbon Ion Irradiation via Periostin on Breast Cancer Cell Invasion of the Microenvironment. J Radiol Radiat Ther 4(1): 1060.